Supplementary Information
Influence of Silver Ion Release on the Inactivation of Antibiotic Resistant Bacteria using Light-Activated Silver Nanoparticles

Adeola Julian Sorinolu[1#], Varsha Godakhindi [2,3#], Paolo Siano[2], Juan L. Vivero-Escoto[2,3]*, and Mariya Munir[1]*

[#]Equal contributors

*Corresponding authors: JVE: jviveroe@uncc.edu, (704)-687-5239; MM: mmunir@uncc.edu, 704-687-1623

[1]Department of Civil and Environmental Engineering, University of North Carolina Charlotte, Charlotte, NC, 28223, USA.

[2]Department of Chemistry, University of North Carolina Charlotte, Charlotte, NC, 28223, USA.

[3]Nanoscale Science program, University of North Carolina Charlotte, Charlotte, NC, 28223, USA.

Materials and Methods

The following chemicals and biological media were purchased from various suppliers: concentrated hydrochloric acid (Macron chemicals), nitric acid (Macron chemicals), protoporphyrin IX (Enzo Lifesciences). Polyethyleneimine (PEI) (branched, 10 kDa; Beantown chemicals), 1-Ethyl-3-(3-dimethylaminopropyl) carbodiimide hydrochloride (EDC) (Oakwood Chemicals), silver nitrate ($AgNO_3$), silver standard, cysteamine hydrochloride, N-hydroxysuccinimide (NHS), dimethylamino pyridine (DMAP), N,N-Diisopropylethylamine (DIPEA), trisodium citrate dihydrate, 9,10 dimethyl anthracene, 1X phosphate buffer saline solution (10 mM) (all from Sigma Aldrich), tannic acid (95%, Acros Organics), dimethyl sulfoxide, dimethylformamide (VWR chemicals) and dichloromethane (Alfa aesar), Nano-W

negative stain (NanoProbes), Roswell Park Memorial Institute (RPMI) media, Fetal Bovine Serum (FBS), penicillin-streptomycin (pen-strep), 1X Dulbecco's phosphate buffer saline (DPBS) (all from Corning), Luria Bertani (LB) broth, LB agar (VWR Life Science). All chemicals were of reagent grade purity or higher and were used as received. Biological media are certified nuclease-free.

Synthesis of thiol functionalized PpIX (cysPpIX).

The synthesis of cysPpIX is carried through a two-steps reaction as illustrated in Scheme S1. PpIX was initially modified to obtain the succinimide ester derivative (sePpIX) according to the following protocol; 112.5 mg of PpIX (0.2 mmol), 184.2 mg of N-hydroxysuccinimide (NHS) (1.6 mmol), 48.9 mg of dimethylamino pyridine (DMAP) (0.4 mmol) and 306.8 mg of 1-Ethyl-3-(3-dimethylaminopropyl) carbodiimide (EDC) (1.6 mmol) were dissolved in a mixture of 10 mL dimethylsulfoxide and dichloromethane (DMSO:DCM; 1:1 vol.) and stirred at room temperature for 48 h. The sePpIX was obtained via precipitation of the reaction using a mixture of ethanol: water (20:80 %v) and separated using vacuum filtration. The obtained precipitate was dried under vacuum condition and stored at –20 °C.

The sePpIX was further functionalized with cysteamine to afford a thiol functionalized PpIX. Briefly, 40 mg of sePpIX (0.05 mmol), 23 µL of N, N-Diisopropylethylamine (DIPEA) (0.132 mmol) and 15 mg of cysteamine-HCl (0.132 mmol) were mixed in 672 µL of DMSO. This mixture was stirred at 80 °C for 96 h. Following this, the desired product (cysPpIX) was purified using a mixture of ethanol:water (20:80 %v) and dried under vacuum condition.

Characterization

The size and morphology of the synthesized nanoparticles were analyzed using transmission electron microscopy (TEM, JEM 1230) operating at an accelerating voltage of 200 kV. The samples were prepared by dispersing AgNPs and PpIX-AgNPs in 50 µL of ethanol. Then, 10 µL of the sample was placed on the carbon coated copper grid and air dried for 1-2 h. The nanoparticle size and its distribution were calculated using ImageJ software. Sample size of 150 nanoparticles was considered for analysis and size was finally reported as average ± sd.

PEI-PpIX-AgNP (15 ng/µL) in water was well sonicated and 10 µL of the sample was placed on the carbon coated copper grid. After 1-minute, excess sample was wicked off (not to dryness)

using filter paper. A single drop (5 uL) of Nano-W stain was added to the grid and excess sample was wicked off after 1-minute. This step was repeated again, and the final grid was air dried for 24 h at room temperature. The nanoparticle size and its distribution were calculated using ImageJ software. Sample size of 100 nanoparticles was considered for analysis and final distribution was plotted as a histogram.

Post irradiation TEM analysis was performed for AgNPs, PpIX-AgNPs and PEI-PpIX-AgNPs in water and PBS at time points: 0 h, 20 min and 24 h. Petri dishes containing individual samples were irradiated with a white light source (400-700 nm; 56 ± 2 mW/cm^2) for 20 min. Then, 200 µL of aliquots were collected at time points 20 min and 24 h. The collected aliquots were immediately centrifuged for 10 min at 13000 rpm and the pellet was used for TEM analysis. The pellet obtained was sonicated for 5 min and 10 µL of this sample was placed on the carbon coated copper grid. After 5 min, excess volume was wicked off using filter paper and the grids were dried in the oven for 2 h at 150 °C.

Hydrodynamic size, polydispersity index (PdI) as well surface charge determination was performed using Malvern ZetaSizer. UV-Vis spectra were obtained using Cary 300 Bio UV-Visible spectrophotometer (Varian). 3 mL of sample and reference solvent (DMF) was used to obtain absorbance spectra from 200-800 nm. Furthermore, chemical changes confirming PpIX modifications were analyzed using MALDI-MS, ^{1}H NMR and FTIR.

sePpIX: ^{1}H NMR (300 MHz, DMSO-d_6, ppm): δ 2.74 (s, 8H), 3.17 (t, 4H), 3.64-3.77 (s, 12H), 4.50 (t, 4H), 6.44-6.50 (dd, 4H), 8.48-8.60 (m, 2H), 10.27-10.38 (4s, 4H). FT-IR (cm^{-1}): 3318 (N-H), 2947 (C-H), 1810 (C=O), 1778 (C=O), 1739 (C=O), 1627 (CN); MALDI-MS (m/z): Calculated: [M]+ = 756.30; Observed: [M+2]+ = 758.44.

cysPpIX: ^{1}H NMR (300 MHz, DMSO-d_6, ppm): 3.19 (t, 4H), 3.59-3.63 (dd, 12H), 3.72 (m, 4H), 4.03 (m, 2H), 4.34 (t, 4H), 6.19-6.44 (dd, 4H), 8.16-8.43 (m, 2H), 10.18-10.29 (d, 4H). IR (cm^{-1}): 3312 (N-H), 2913 (C-H), 1741 (C=O), 1643 (C-N). Calculated: [M]+ = 680.29; Observed: [M-2] + = 678.90.

Photophysical characterization of PpIX conjugated AgNPs was performed by determining the $^1O_2$ quantum yield (Φ_Δ) [1]. Singlet oxygen generation was quantified by monitoring the absorbance decay of 9,10 dimethylanthracene (DMA). The following protocol was carried put; 1 mL of 5 µM

of PS in DMF (PpIX, cysPpIX and PpIX-AgNPs) was mixed with 1 mL of 50 μM of DMA in DMF in quartz cuvettes (1cm x 1cm). Extreme care was taken to not expose the mixture to any light. This mixture was irradiated at 515 nm for varying time interval (0, 1, 2, 5, 10, 20 and 30 min) using a spectrofluorometer (Shimadzu RF 5301). The decay in absorbance 380 nm was monitored by measuring its UV-Vis spectra immediately after light irradiation and was plotted against the irradiation time. TPP in DMF was used as the reference ($\Phi_\Delta = 0.62$).

MDR *E. coli* Library Preparation and Sequencing

A single bacterial colony of each strain was aseptically picked from the top of a LB agar plate using a sterile loop and inoculated into sterile LB broth media supplemented with tetracycline, ampicillin and sulfamethoxazole-trimethoprim at 50, 100 and 200 μg/mL respectively. Bacteria cells were grown overnight (~ 18 hours) at 37 °C under continuous gentle mixing at 200 rpm. Overnight cells were harvested the following day by centrifugation at 7000 rpm for 5 min. Genomic DNA was extracted using QIAamp® DNA Mini kit (QIAGEN) following the manufacturer's protocol for bacterial extraction. The extracted DNA sample was quantified using Qubit® 3.0 fluorometer (3.0) based on the Qubit dsDNA HS Assay (Thermo Scientific™). The purity of the DNA was confirmed by measuring the concentration using a Nanodrop™ UV-Vis spectrophotometer (Thermo Scientific™). The concentration and A260/A280 were 65.8 ng/μL and 2.02 respectively and confirmed to be of high purity for sequencing application. Sequencing was carried out on PromethION48 (Oxford Nanopore Technologies) using the SQK-LSK-109 ligation sequencing kit. This MDR *E. coli* sample was sequenced alongside 14 other bacteria isolates for use in another study. Thus, EXP-NBD196 native barcoding was used for the pooled sequencing run to identify individual samples. The library preparation step, barcode ligation, adapter ligation and clean up, followed the Nanopore Native barcoding genomic DNA with EXP-NBD196 and SQK-LSK-109 (version NBE_9129_v109_revB_19Jan2021). For all isolates, 400 ng gDNA was used. DNA fragmentation step was not included in the protocol and Longer DNA fragments were enriched by washing pooled barcoded sample beads with long fragment buffer (LFB). The concentration of pooled DNA samples quantified after the adapter ligation and clean-up was obtained as 23.8 ng/μL. A volume of 12 μL DNA library was added to a mixture of loading beads and sequencing buffer and loaded unto a new PromethION flow cell (FLO-PRO112). The flow cell used passed the flow cell check and it was primed before loading samples whilst

observing standard procedure to prevent the introduction of air bubbles. In all library preparation steps, LoBind consumables (Eppendorf) were used and nuclease-free certified reagents as recommended in the protocol.

MDR *E. coli* Sequence Data Analysis, Classification and Identification

For the MDR *E. coli* (barcode 1), 378,283 total reads were analyzed and 343,575 were successfully aligned to NCBI complete genomes. Implementing a 1% abundance cutoff, the most abundant species in this mixed sample were *E. coli, S. aureus, P. fermentans, K. pneumoniae, P. aeruginosa,* and *L. granuli* with 158,479, 72,002, 22,492, 13,733, 6,043, and 3,503 reads respectively. For *E. coli,* 154,686 reads were species classified and the remaining reads were split amongst 112 child taxa/strains, with the largest amount of hits belonging to the CE10 strain.

Of this *E. coli* portion of reads, 11,775 aligned to 327 unique entries in the Comprehensive Antibiotic Resistance Database (CARD) with an average accuracy of 91.4%. The highest abundance ARG entry was APH (3')-Ia; a transposon-encoded aminoglycoside phosphotransferase with 837 aligned reads. This was followed by *E. coli* rrsH gene modifications at 458 reads conferring resistance to spectinomycin in K-12 strains, and rpoB at 198 reads conferring resistance to rifampicin in O157 strains.

SCHEMES

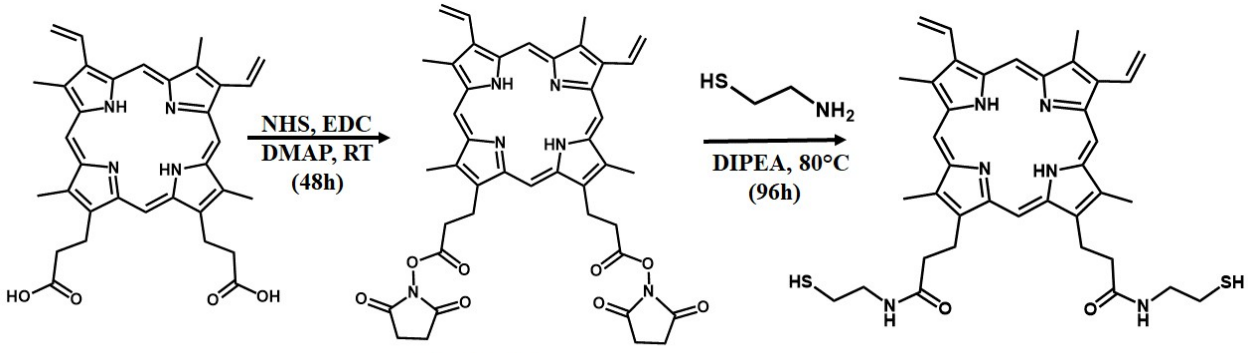

Scheme S1. Synthesis of cysPpIX following a two-steps approach. First, the carboxylic acid groups in PpIX were activated using NHS followed by the nucleophilic acyl substitution reaction using cysteamine.

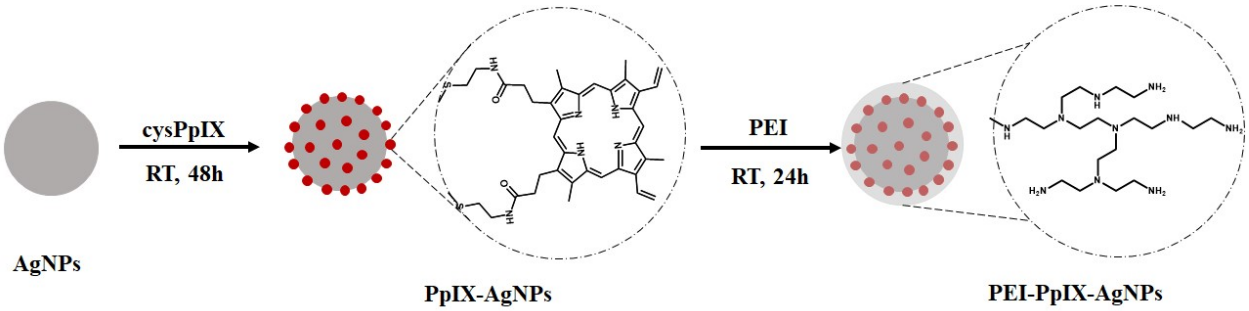

Scheme S2. Fabrication of PpIX-AgNPs and PEI-PpIX-AgNPs.

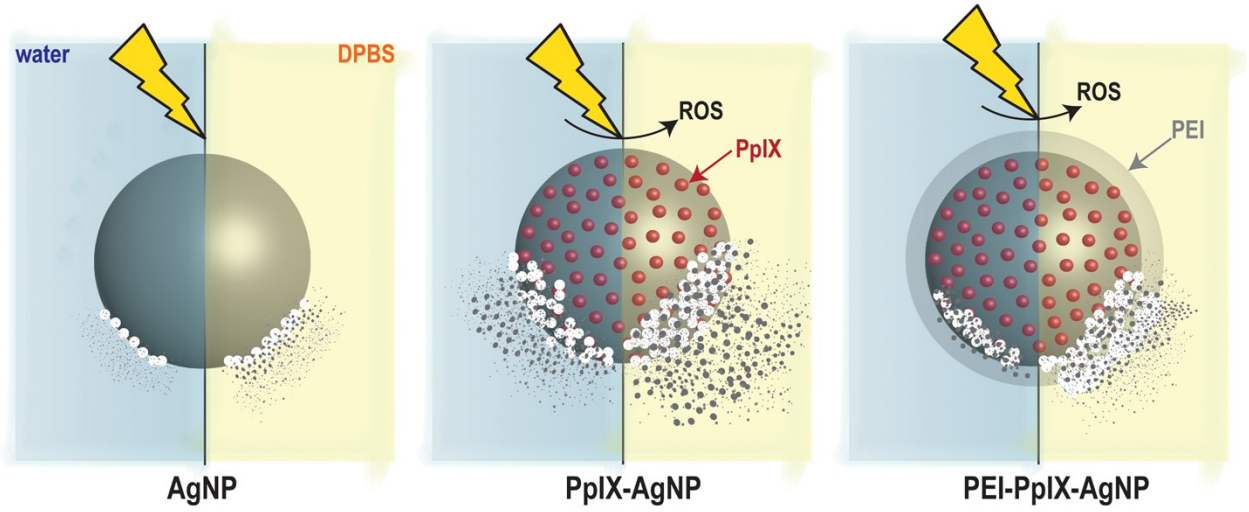

Scheme S3. Schematic representation of the degradation of AgNPs, PpIX-AgNPs and PEI-PpIX-AgNPs in the presence of light in water or DPBS conditions. AgNPs are usually degraded by the medium regardless the presence or absence of light. The ions in DPBS increase the solubility of Ag^{+}, which results in the enhancement of the degradation of AgNPs. The presence of the PpIX photosensitiser upon light irradiation accelerates the degradation of AgNPs. The presence of PEI polymer partially inhibits the degradation of AgNPs.

FIGURES

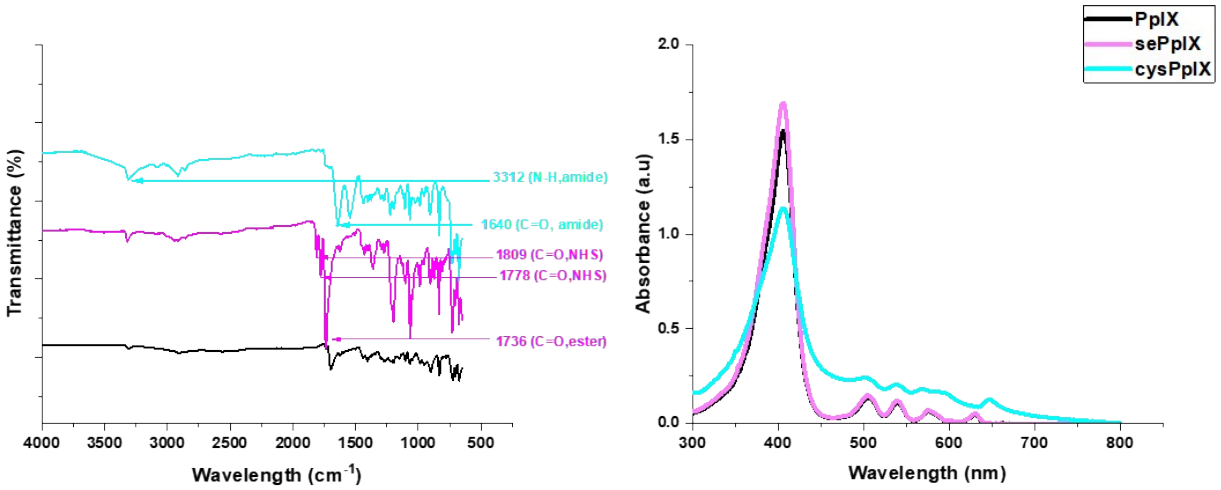

Figure S1. (a) FT-IR and **(b)** UV-Vis (DMF) spectra for PpIX (black), sePpIX (pink) and cysPpIX (blue).

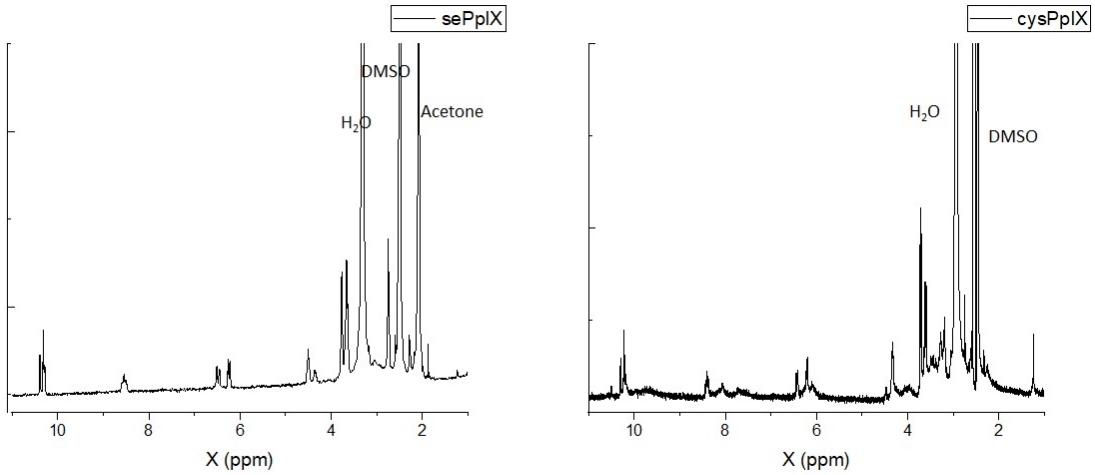

Figure S2. ^{1}H-NMR spectra for sePpIX and cysPpIX.

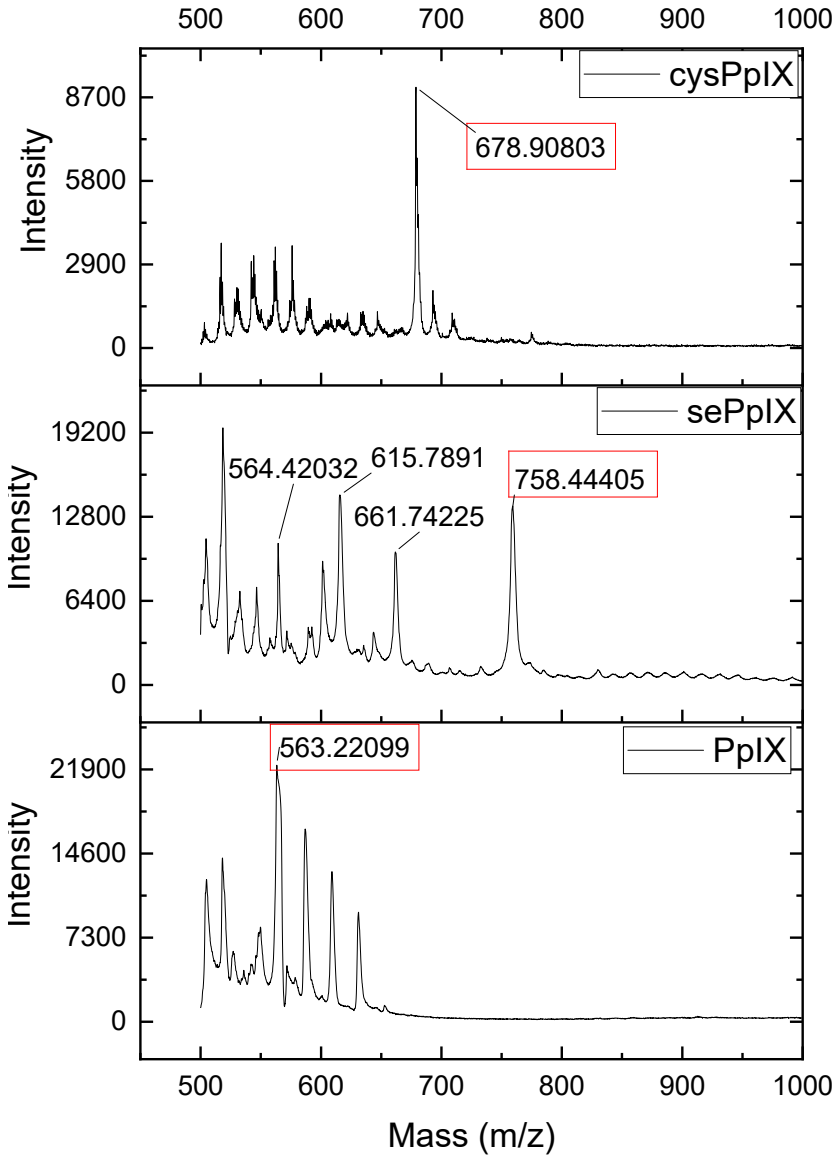

Figure S3. MALDI-MS spectra for PpIX, sePpIX and cysPpIX. Expected m/z: $[PpIX]^+$ = 562.25 / Observed: m/z: $[PpIX+1]^+$ = 563.22; Expected m/z: $[sePpIX]^+$ = 756.30/Observed: m/z: $[sePpIX+2]^+$ = 758.44; Expected m/z: $[cysPpIX]^+$ = 680.29/ Observed: m/z: $[cysPpIX-2]^+$ = 678.90.

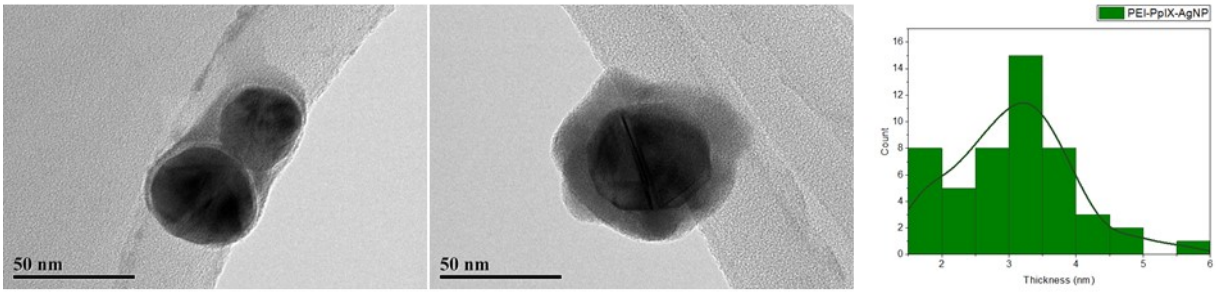

Figure S4. TEM image of PEI-PpIX-AgNPs negatively stained to show the presence of PEI. The thickness of PEI shell was measured using the TEM images obtaining an average of 3.0 ± 0.9 nm (n=50).

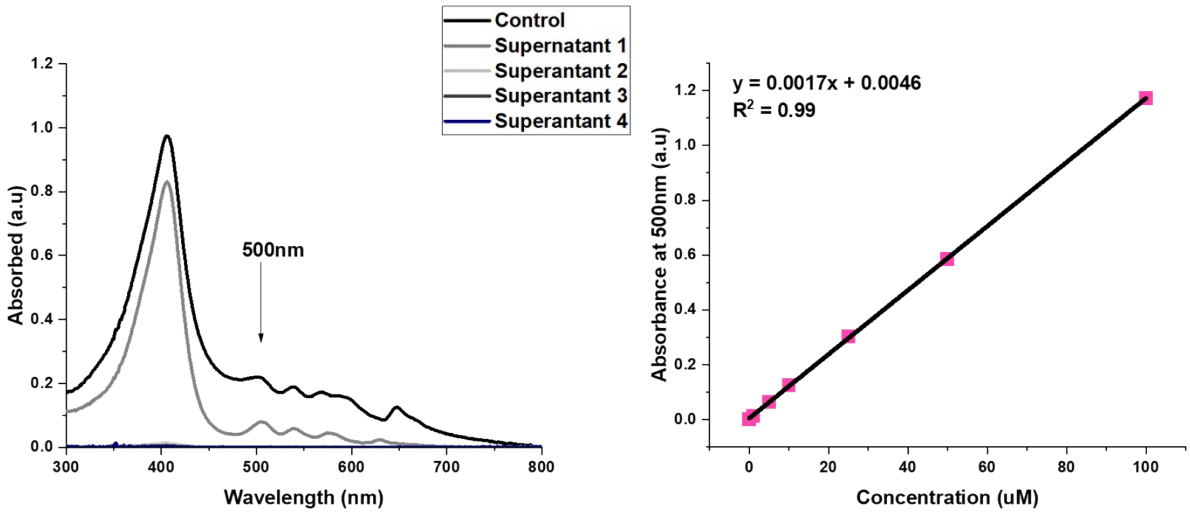

Figure S5. (left) UV-Vis plot for supernatants collected before (control) and after (Supernatant 1-4) the reaction between cysPpIX and AgNP. (right) Calibration curve for the quantification of cysPpIX on AgNP.

Equation 1

$$\%\ PpIX\ loaded = \frac{cysPpIX\ before\ reaction(mg) - cysPpIX\ in\ the\ supernatants, S1 - S4\ (mg)}{cysPpIX\ before\ reaction\ (mg)}$$

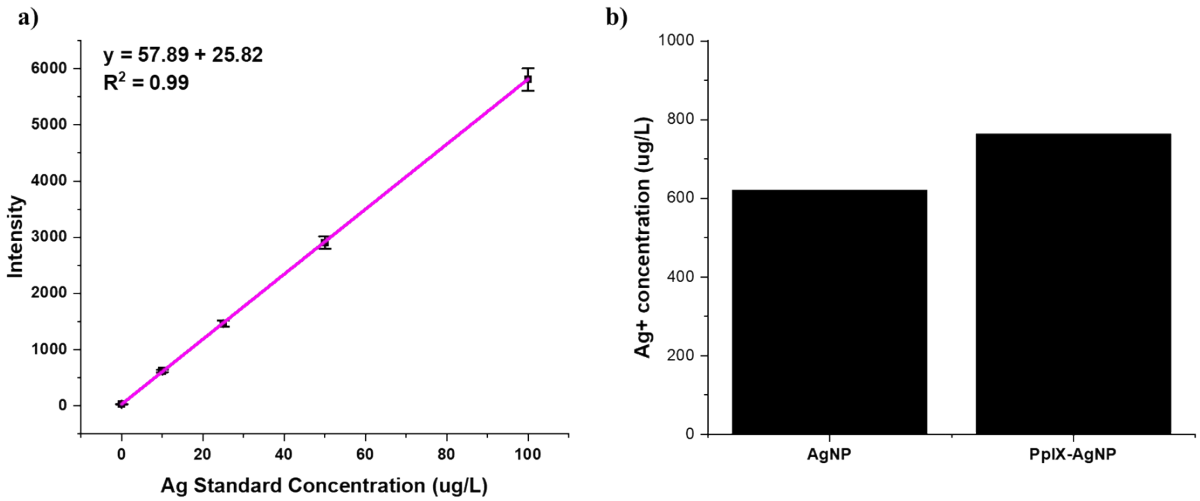

Figure S6. a) Calibration curve for Ag^+ digestion and release experiments. b) Maximum Ag^+ in 1.5 µg/mL of AgNP and PpIX-AgNP obtained after digestion.

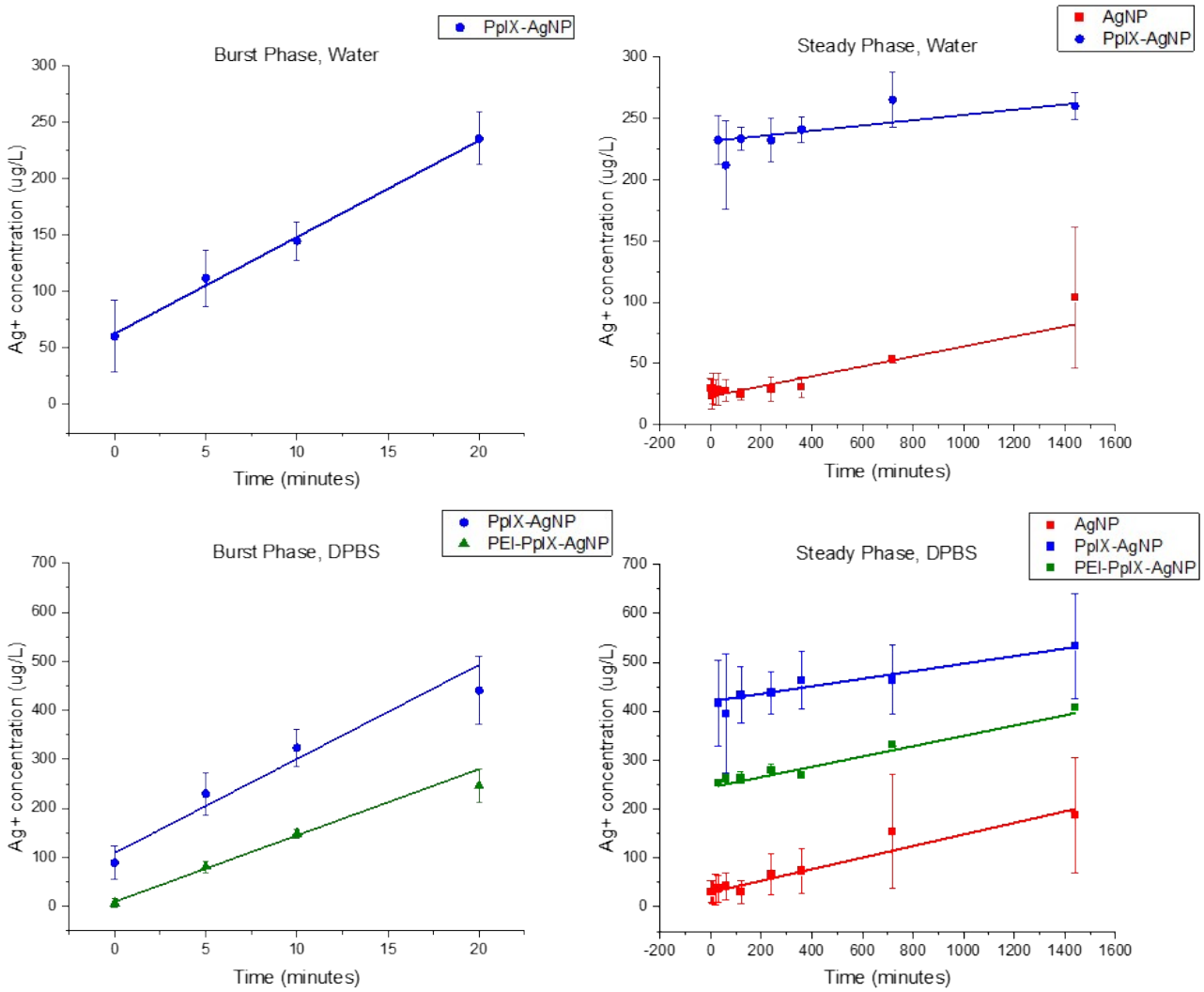

Figure S7. Kinetic release linear fitted plots for AgNP, PpIX-AgNP and PEI-PpIX-AgNP in water and DPBS represented as burst and steady release phase.

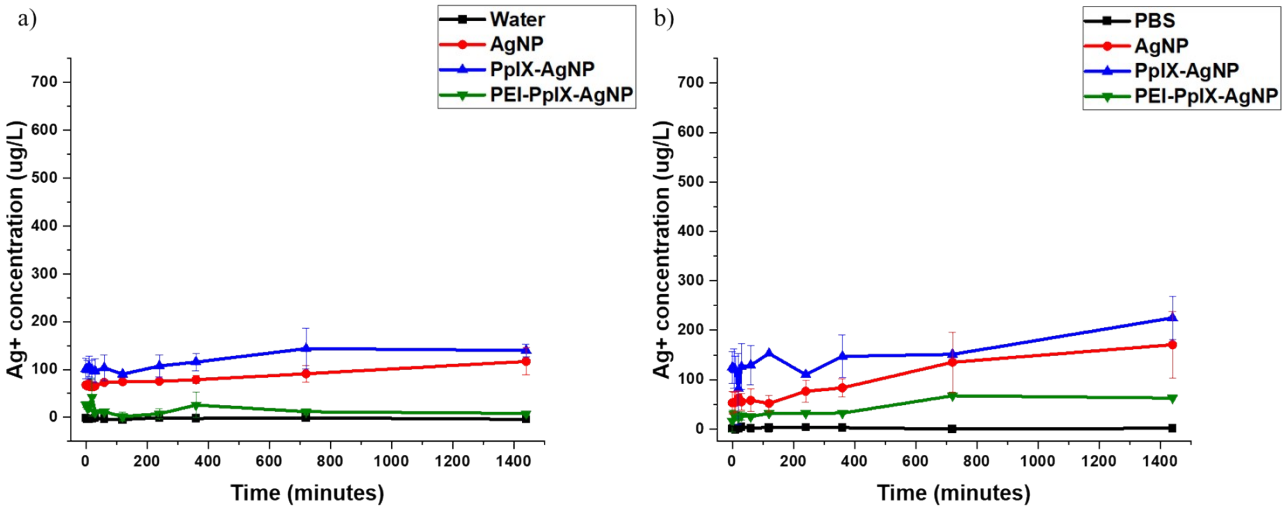

Figure S8. Ag^{+} release kinetics in the absence of light for AgNPs, PpIX-AgNPs and PEI-PpIX-AgNPs measured in a) water and b) DPBS.

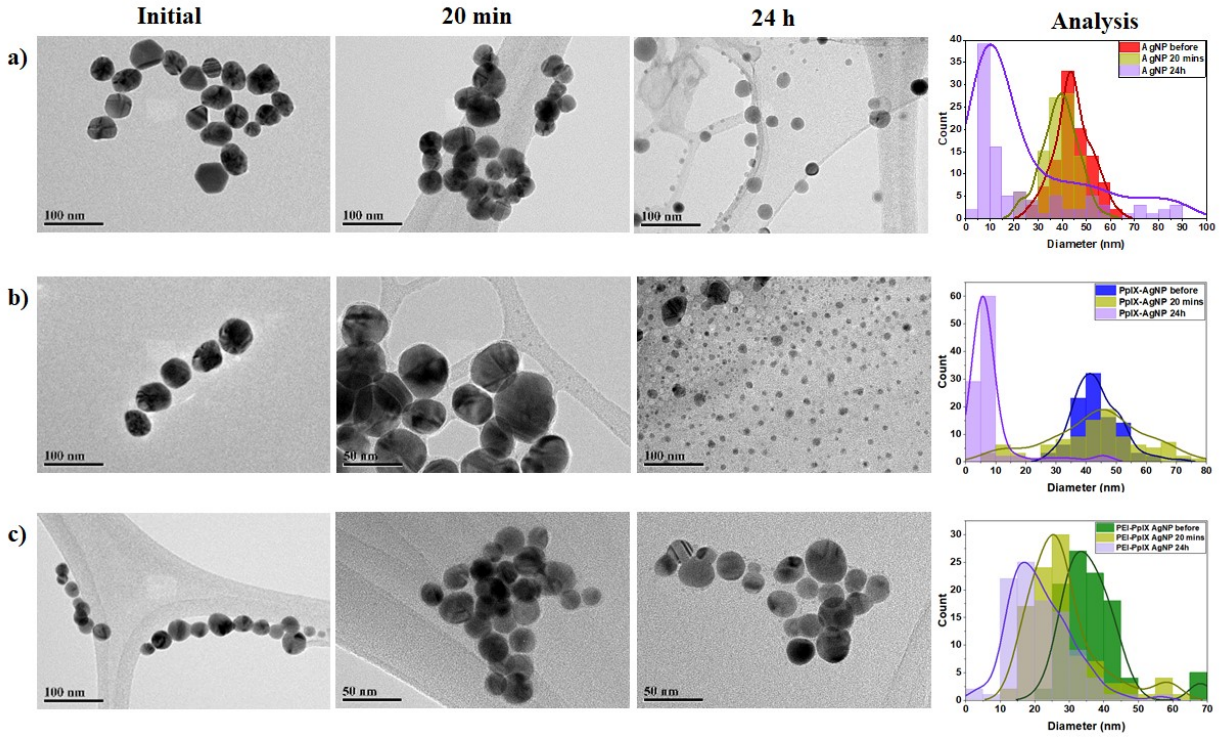

Figure S9. TEM images and quantification of the degradation of a) AgNPs, b) PpIX-AgNPs and c) PEI-PpIX-AgNPs in water post-light irradiation at 20 min and 24 h. Nanoparticles diameter was measured using Image J and plotted to determine the change in size distribution (n = 100).

Equation 2

$$\%\ Ag+\ release = \frac{Ag+\ released\ at\ time\ point\ 't'\ (\frac{\mu g}{L})}{Total\ Ag+\ digested\ (\frac{\mu g}{L})}$$

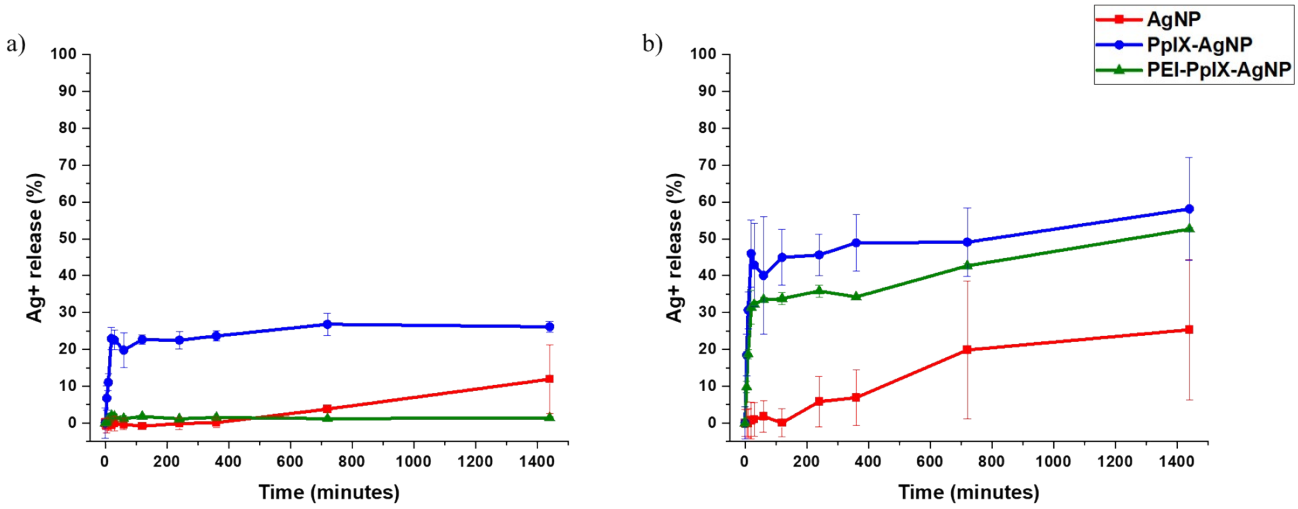

Figure S10. Ag^{+} release kinetic in a) water and b) DPBS expressed in % using the total amount of Ag in the nanoparticles for AgNPs, PpIX-AgNPs and PEI-PpIX-AgNPs. Ag+ release percentage was calculated using equation 2.

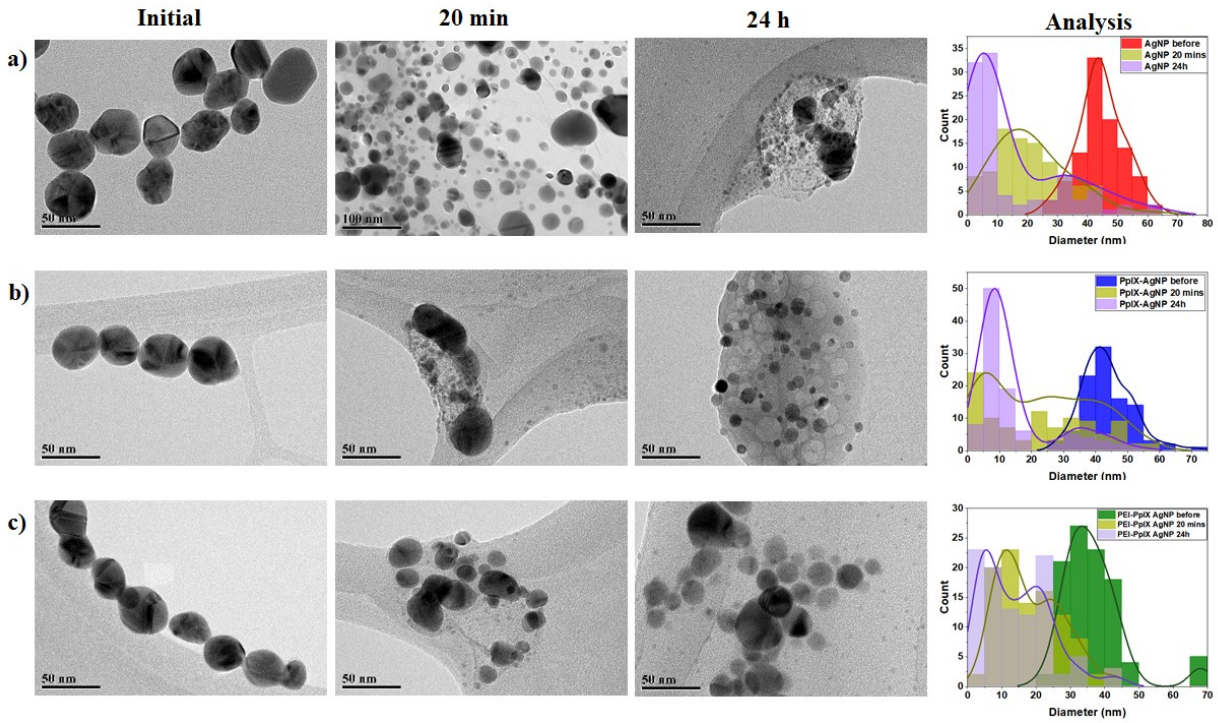

Figure S11. TEM images and quantification of the degradation of a) AgNPs, b) PpIX-AgNPs and c) PEI-PpIX-AgNPs in DPBS post-light irradiation at 20 min and 24 h. Nanoparticles diameter was measured using Image J and plotted to determine the change in size distribution (n = 100).

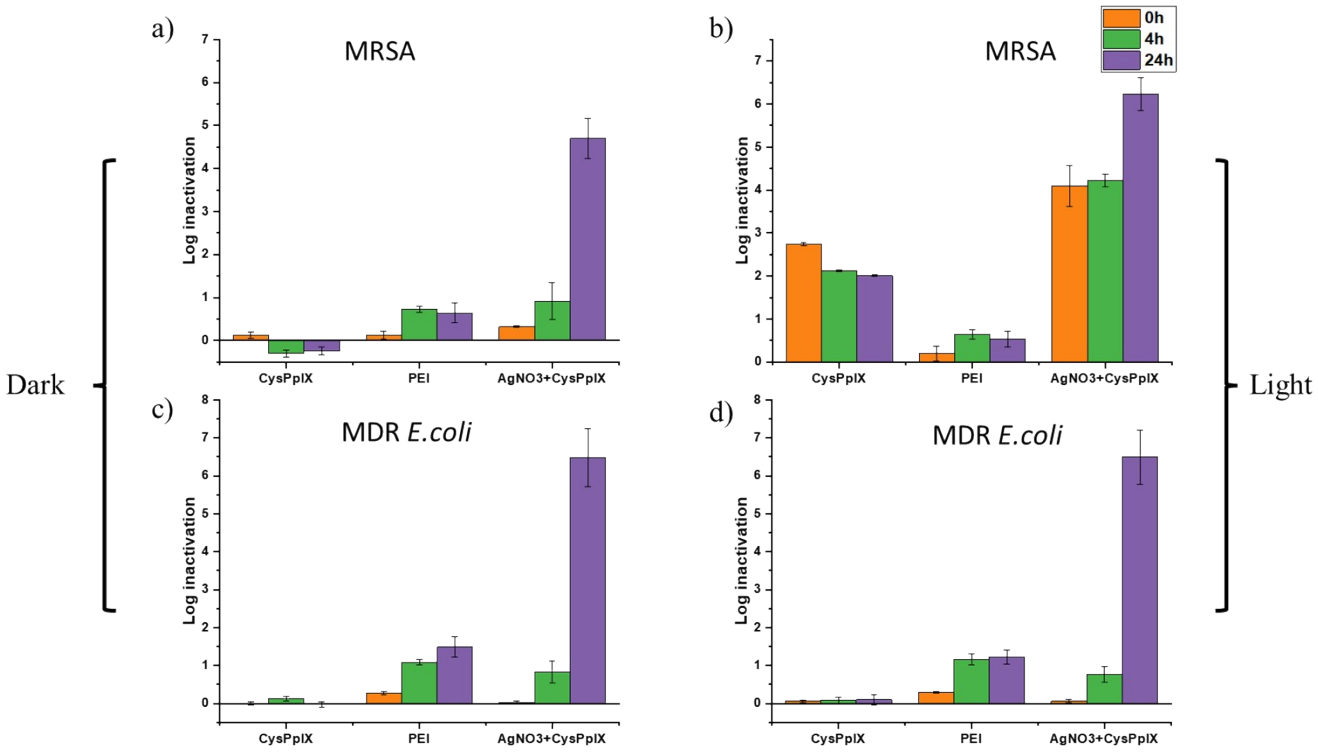

Figure S12. Antibacterial activity of controls tested in MRSA and MDR *E. coli* under light and dark conditions.

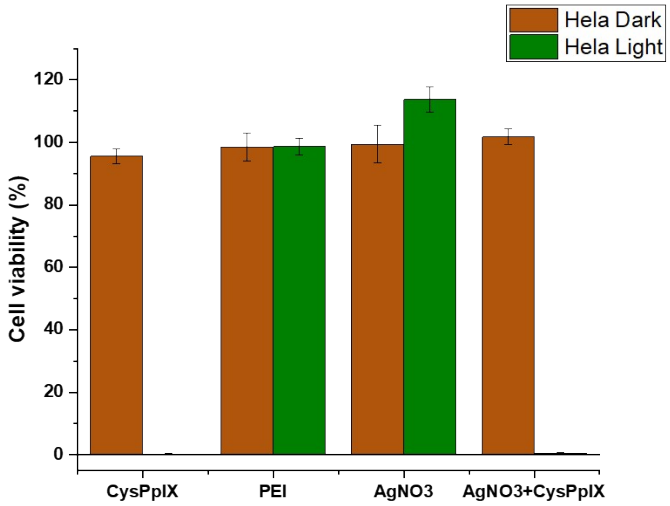

Figure S13. Cytotoxicity of the controls (cysPpIX, AgNO3, cysPpIX+AgNO3, PEI) tested in Hela cells in the presence (light) and absence (dark) of blue light.

TABLES

Table S1. ICP-OES digestion results for AgNPs, PpIX-AgNPs and PEI-PpIX-AgNPs.

Sample	**Digested Ag^+ (ug)**	**Ag^+ per ug of NP (%)**
AgNP	48.9 ± 1.8	97.77
PpIX-AgNP	28.8 ± 2.6	57.60
PEI-PpIX-AgNP	15.0 ± 0.7	29.92

Table S2. Summary of hydrodynamic size/polydispersity index (PdI) and ζ-potential for AgNPs, PpIX-AgNPs and PEI-PpIX-AgNPs.

Sample Name	Hydrodynamic Size (nm)	PdI	Z- potential (mV)
AgNP	36.34 ± 1.11	0.2	-49.08 ± 5.48
PpIX-AgNP	55.60 ± 6.68	0.43	-57.28 ± 4.77
PEI-PpIX-AgNP	137.59 ± 3.99	0.29	27.11 ± 1.71

Table S3. Singlet oxygen quantum yield analysis (Φ_Δ) using TPP (DMF) as the reference (Φ_Δ = 0.62). λ_{ex} = 515nm.

Sample	**Φ_Δ**
PpIX	0.60
CysPpIX	0.38
AgNP-PpIX	0.01

Table S4. Summary of linear fitting parameters for AgNP, PpIX-AgNP and PEI-PpIX-AgNP.

			Slope	R^2
AgNP	Water		0.04	0.92
	DPBS		0.12	0.87
PpIX-AgNP	Water	Burst Phase	8.56	0.99
		Steady Phase	0.02	0.81
	DPBS	Burst Phase	19.18	0.95
		Steady Phase	0.08	0.87
PEI-PpIX-AgNP	DPBS	Burst Phase	13.53	0.99
		Steady Phase	0.11	0.92

Determination of the number of PpIX molecules per silver nanoparticle

By assuming that AgNPs are spherical in shape, the mass of each nanoparticle (m_{AgNP}) was calculated based on average diameter determined from TEM and density value obtained from Tadjiki et al [2]. The number of PpIX molecules per nanoparticle was calculated using the Equation (3).

Equation 3

$$PpIX\ molecules\ per\ AgNP = \frac{m_{AgNP}\, x\, Mf_{(PpIX:AgNP)}\, x\, N_a}{MW_{cysPpIX}}$$

Where, m_{AgNP} is the mass of each AgNP, Mf is mass fraction PpIX:AgNP (0.45:0.55 = 0.818) for PpIX-AgNP, N_a is the Avogadro's constant and $MW_{cysPpIX}$ is the molecular weight of cysPpIX.

References

1. Hurst AN, Scarbrough B, Saleh R, Hovey J, Ari F, Goyal S, Chi RJ, Troutman JM, Vivero-Escoto JL. Influence of Cationic meso-Substituted Porphyrins on the Antimicrobial Photodynamic Efficacy and Cell Membrane Interaction in Escherichia coli. International Journal of Molecular Sciences. 2019;20(1). doi: 10.3390/ijms20010134. PubMed PMID: WOS:000459747700134.

2. Tadjiki S, Montaño MD, Assemi S, Barber A, Ranville J, Beckett R. Measurement of the Density of Engineered Silver Nanoparticles Using Centrifugal FFF-TEM and Single Particle ICP-MS. Analytical Chemistry. 2017;89(11):6056-64. doi: 10.1021/acs.analchem.7b00652.